Estudios Geológicos
enero-junio 2024, 80(1), 1075
ISSN-L: 0367-0449
https://doi.org/10.3989/egeol.45173.1075

The 2011-2012 Puyehue-Cordón Caulle (Southern Andes) tephra deposit: influence of the number of field measurements on isopach drawing and volume estimate

El depósito de caída de tefra de la erupción de 2011-2012 del Complejo Volcánico Puyehue-Cordón Caulle (Andes del Sur): Influencia del número de mediciones de campo en la construcción de isopacas y la estimación del volumen

Jorge E. Romero[1]*, Diego I. Gallardo[2], Juan J. Gaitán[3], Frederick J. Swanson[4], Florencia Sánchez[5], Marcela Saavedra[6], Nikolas Zambrano[6], Hannah Buckland[7], Inés Rodríguez[6]

1 Instituto de Ciencias de la Ingeniería, Universidad de O'Higgins, Libertador Bernardo O'Higgins 611, Rancagua, Chile. https://orcid.org/0000-0001-9383-9830, jorge.romero@uoh.cl
2 Departamento de Estadística, Facultad de Ciencias, Universidad del Bío-Bío, Concepción 4081112, Chile. https://orcid.org/0000-0001-8184-7403, dgallardo@ubiobio.cl
3 Laboratorio de Teledetección - SIG, Instituto de Suelos -INTA Castelar. Nicolás Repetto y de los Reseros S/N CP 1686, Hurlingham, Buenos Aires, Argentina. https://orcid.org/0000-0003-2889-1418, jgaitan@unlu.edu.ar.
4 U.S. Department of Agriculture, Forest Service, Pacific Northwest Research Station, Corvallis Forestry Sciences Laboratory, 3200 Jefferson Way, Corvallis, OR 97331, USA https://orcid.org/0000-0001-9690-2428, fjswanson541@gmail.com.
5 Institute of Earth Sciences, Pole of the University of Minho, Braga, Portuga. flsanchezr@udd.cl. https://orcid.org/0009-0001-8683-3833
6 Departamento de Geología y Obras Civiles, Universidad Católica de Temuco, Temuco, Chile. https://orcid.org/0000-0002-4323-2413, marcela.saavedra2016@alu.uct.cl; https://orcid.org/0000-0003-3493-6643, nzambrano2016@alu.uct.cl; https://orcid.org/0000-0002-5398-4176 irodriguez@uct.cl;
7 Department of Geography, Faculty of Science and Engineering, Swansea University, Swansea, United Kingdom https://orcid.org/0000-0002-9954-4993;
* Corresponding author: jorge.romero@uoh.cl

ABSTRACT

Estimating tephra fall volumes is critical for assessing the impacts of explosive eruptions and calculating eruption source parameters (ESPs). Estimates are subject to uncertainties that span from measuring deposit thicknesses to the different volume integration models implemented. In this sense, the number of field control points (FCPs) may produce variable volume outputs. In this contribution, we use a high-resolution dataset consisting of 270 FCPs to assess the 2011-2012 Puyehue-Cordón Caulle sub-Plinian tephra volume (previously estimated at 0.5-1.5 km^3). We used a suite of randomly selected sub-datasets of FCPs ranging from 10 to 250. Hand-drawn isopachs were then integrated by the exponential and Weibull methods, with the goal of determining a minimum sample size to obtain volume estimation with little or no variation compared to the full dataset. Obtained bulk volumes range from 0.91 to 22.7 km^3. However, the estimates converge to 1.15 ± 0.05 km^3 when all the dataset is used, which is similar to results using c. 400 FCPs in the literature. Therefore, datasets of 89 and 60 samples for exponential and Weibull models, respectively, yield tephra fall volume estimates similar to considering the whole dataset. Notably, a small number of FCPs (50-70) generally produces volume overestimation to ≥30 % using the exponential method. Increasing FCPs yield more accurate isopach maps, while data distribution is important for volume uncertainty as medial observations account for larger volumes than the distal ones. These results provide new insights on the uncertainties associated with interpreting ESPs from tephra fall deposits.

Keywords: Tephra fall deposit; Puyehue-Cordón Caulle; Southern Volcanic Zone; Andes; Chile; Argentina.

Recibido el 14 de septiembre de 2023; Aceptado el 5 de diciembre de 2023; Publicado online el 2 de octubre de 2024

Citation / Cómo citar este artículo: Romero, J.E., et al. (2024). The 2011-2012 Puyehue-Cordón Caulle (Southern Andes) tephra deposit: influence of the number of field measurements on isopach drawing and volume estimate. Estudios Geológicos, 80(1), 1075. https://doi.org/10.3989/egeol.45173.1075

RESUMEN

La estimación de los volúmenes de caída de tefra es fundamental para evaluar los impactos de las erupciones explosivas y el cálculo de los parámetros eruptivos de la fuente (PEF). Las estimaciones están sujetas a incertidumbres que abarcan desde la medición del espesor de los depósitos hasta los diferentes modelos de integración de volúmenes implementados. En este sentido, el número de puntos de control de campo (NPCs) puede producir resultados de volumen variables. En esta contribución, utilizamos un conjunto de datos de alta resolución consistente en 270 NPCs para evaluar el volumen aparente de tefra sub-Pliniano de Puyehue-Cordón Caulle 2011-2012 (previamente estimado en 0,5-1,5 km^3). Se utilizó un conjunto de sub-datos seleccionados aleatoriamente de NPCs que oscilaban entre 10 y 250. A continuación, se integraron isopacas dibujadas a mano mediante los métodos exponencial y de Weibull, con el objetivo de determinar un tamaño de muestra mínimo para obtener una estimación estable del volumen de caída de tefra en comparación con el conjunto de datos completo. Los volúmenes obtenidos oscilan entre 0,91 y 22,7 km^3 aunque convergen en 1,15±0.05 km^3 cuando se utiliza todo el conjunto de datos, lo que es similar a los resultados obtenidos utilizando ca. 400 NPCs en la literatura. Por lo tanto, los conjuntos de datos de 89 y 60 puntos para los modelos exponencial y Weibull, respectivamente, arrojan estimaciones del volumen de caída de tefra similares al conjunto de datos completo. En particular, un pequeño número de NPCs (50-70) generalmente produce una sobreestimación del volumen ≥30% usando el método exponencial. El aumento de NPCs produce mapas de isopacas más precisos, mientras que la distribución de los datos es importante para la incertidumbre del volumen, ya que las observaciones mediales representan volúmenes mayores que las distales. Los resultados aportan una nueva visión sobre las incertidumbres asociadas a la interpretación de los PEFs de los depósitos de caída de tefra.

Palabras clave: Puyehue-Cordón Caulle; Depósito de caída de tefra; Zona Volcánica Sur; Andes; Chile; Argentina.

Introduction

Estimating the volume of tephra fall deposits is a recurrent problem in physical volcanology. Mapping the thickness, density, and mass accumulation of tephra fall deposits provides the necessary information for estimating the bulk and dense rock equivalent (DRE) volume and mass which are key eruption source parameters (ESPs) for explosive volcanic eruptions (Pyle et al. 2015; Bonadonna et al. 2015a; Spanu et al. 2016; Biass et al. 2019; Bonadonna et al., 2022). Eruption volume estimates are also necessary for models of volcanic ash transport, assessments of the risk from ash to infrastructure (roof collapse, road marking visibility), and environmental concerns. Tephra quantification represents a first response to the impacts of these eruptions. Therefore, for the management of the affected areas and the evaluation of the environmental, social, and economic impacts, it is essential to carry out a best-guess estimation of the volume and spatial distribution of tephra deposits.

Variable erupted volume estimates may be a consequence of the complex spatial variability of the deposit thickness (e.g., Engwell et al., 2013; Buckland et al., 2020), field measurement uncertainty (Engwell et al. 2013), influence of isopach draftsmanship (Klawonn et al. 2014), isopach geometry (Bernard et al. 2013), extrapolation of data (Yang and Jenkins, 2023), and the incomplete sampling of tephra deposits (e.g., Andronico et al. 2014; Engwell et al. 2015; Green et al. 2016; Primerano et al. 2021; Constantinescu et al. 2022a, b). Also, the different integration methods applied to volume estimates have influence on these estimates (Pyle 1989; Fiersten and Nathenson 1992; Legros 2000; Bonadonna and Houghton 2005; Sulpizio 2005; Bonadonna and Costa 2012; Yang and Jenkins, 2023). Andronico et al. (2014) determined that an incompletely sampled Etna tephra fall deposit (medial thickness data only) estimated only 22% of the originally erupted mass for the total deposit. Similarly, bulk volume estimates of the Mazama tephra (Crater Lake, USA) range from 134-224 km^3 simply by using different combinations of field measurements and isopach maps (Buckland et al. 2020). Engwell et al (2015) used the Fogo A deposit to demonstrate a systematic decrease in volume uncertainty when using a larger number of field measurements, and that the volume estimate stabilized when 60 or more thickness measurements were used. These authors also found that random sampling of the field data often under-represents proximal data, meaning that volume estimates are influenced by the spatial distribution of the data. Consequently, uncertainty sources also propagate to the estimation of ESPs (Bonadonna et al. 2015a). However, most studies of uncertainty propagation have been carried out using limited datasets (<100 control points) on small-to-moderate sized eruptions (i.e., Volcanic Explosivity Index, VEI 2-4; Newhall and Self 1982).

In 2011, a sub-Plinian eruption occurred in the Puyehue-Cordón Caulle Volcanic Complex (PCCVC; 40.5°S, 72.2°W) in the Andean Southern Volcanic Zone. The tephra fall from the eruption impacted several Andean regions particularly over the Argentinean Patagonia (e.g., Wilson et al. 2013; Elissondo et al. 2016; Swanson et al. 2016; Romero et al., 2024). Field-based isopachs of the 2011-2012 PCCVC eruption were used to validate the volcanic ash forecast models (e.g., Collini et al. 2013; Tadini et al., 2022), which are relevant for hazard mapping, civil protection, air quality, and aviation. These results have also been used to evaluate the impact of the eruption (e.g., Gaitán et al. (2011a, b; Wilson et al. 2013; Elissondo et al. 2016; Montiel et al., 2022), prompting the intervention and aid to farmers from local to international authorities. Also, tephra distributions and volume estimates of the eruption helped to understand tephra impacts and remobilization events (e.g., Dominguez et al. 2020, 2021; Del Bello et al., 2022). The bulk erupted volume of the tephra fall deposit has been estimated by different authors between 0.5 and 1.5 km^3 (Gaitan 2011; Amigo et al. 2012; Silva et al. 2012; Pistolesi et al. 2015; Alloway et al. 2015; Naranjo et al. 2017).

This paper explores how the number of field control points (FCPs) influences the tephra fall volume estimates. The dataset contains 270 FCPs collected between 2011 and 2018 from the 2011-2012 PCCVC (VEI 5) eruption. This is unlike other studies that have explored the sensitivity of volume estimates to field data distribution that used data from smaller deposits, such as Kīlauea Iki 1959 (Klawonn et al. 2014). The tephra deposit from the 2011-2012 PCCVC eruption is large and widespread, meaning that in some areas, the deposit has been remobilized or is difficult to access. In our contribution, we characterize the general stratigraphy of the deposit to ensure its pristine preservation. However, our main goal is to establish the minimum number of field measurements and associated isopachs required to reach a stable estimate of the tephra fall deposit volume. Moreover, we discuss the sources of variability in the volume estimates when certain sample sizes are used and how this can affect strategies for field data collection following a moderate explosive eruption.

The 2011-2012 Puyehue-Cordón Caulle eruption

Volcanological overview

The PCCVC (40.5°S, 72.2°W) is a cluster of Pleistocene-to-Holocene volcanic vents aligned in NW–SE trend oblique to the main volcanic front of the Chilean Andes Southern Volcanic Zone (SVZ; Fig.1a) (Lara et al. 2006a). Uniquely, the PCCVC erupts high-MgO basalt together with rhyodacite and rhyolite products, unlike those observed in most basaltic and basaltic andesite SVZ volcanoes (López-Escobar et al. 1981; Hickey et al. 1986; Gerlach 1988; Tormey et al. 1991). The products consist of lava flows, lava domes, pumice fall deposits and lahars sourced from at least 27 vents from the Late Pleistocene (16.5 ka) to historical times (Katsui and Katz 1967; Lara et al. 2004, 2006a; Lara and Moreno 2006; Singer et al. 2008).

At least six Holocene tephra fall deposits have been identified from the PCCVC, with bulk volumes ranging from 0.1 to 4.32 km^3 and a magnitude of about 5-6 (VEI 5; Naranjo et al. 2017; Toloza et al. 2020). A series of 0.6-0.7 ka BP sub-Plinian phreatomagmatic eruptions destroyed the summit of Puyehue volcano forming the Mil Hojas sequence, totaling 4.3 km^3 bulk volume (Naranjo et al. 2017; Alloway et al. 2021). In 1921-1922 a sub-Plinian eruption was followed by an effusive stage and erupted *ca.* 0.3 km^3 of DRE volume (Steffen, 1922; Krumm 1923; Katsui and Katz, 1967; Singer et al., 2008). Another sub-Plinian eruption was triggered 38 h after the May 22, 1960, M_w 9.5 earthquake (Veyl, 1960; Katsui and Katz, 1967; Lara et al. 2004, 2006b; Lara and Moreno, 2006; Singer et al. 2008), erupting *ca.* 0.57 km^3 tephra (DRE *ca.* 0.25 km^3; Chapron et al., 2006; Lara et al. 2006a, 2006b). Both eruptions are characterized by rhyolitic to rhyodacitic bulk compositions (68.90-70.01 wt. % SiO_2). The tephra deposits from the two sub-Plinian eruptions are clearly recognizable in outcrops along the 215 international highway as two discrete, decimeter-scale layers containing partially weathered pumice lapilli. Petrological evidence suggests that the historical eruptions have all been fed by the same long-lived mush system (Seropian et al. 2021).

Seismic swarms from a volcano-tectonic source occurred in May 1994, March 1999, and May 2007 (Lara et al. 2006a) and two uplift events occurred within the PCCVC between 2008 and 2010 (Jay et al. 2014). The 2011-2012 explosive eruption began at a site known as “Las Sopas” that formerly produced sulfur emissions, hot springs, steaming-ground, and acid-sulfate alterations (Sepúlveda et al. 2005).

The 2011-2012 eruption

The June 4, 2011, PCCVC eruption was preceded by three ground uplift periods between 2003 and 2010

(Delgado, 2021) and a seismic unrest that began in December 2010 (Basualto et al. 2023). It consisted of an increase in the number and magnitude (M > 3) of volcano-tectonic, long-period, and hybrid seismic events that became shallower (1-4 km depth) until April (Bertin et al. 2015). A source of deformation was observed between March and May 2011, covering 40 km^2 and accounting for a 6 cm uplift (Jay, 2014). In May 2011, the magnitude of earthquakes reached M~4 and one day prior to the eruption their frequency was 25 events per hour (Lara et al. 2012).

The eruption started around 18:45 UTC on June 4, 2011, and initially produced a sustained sub-Plinian eruption column (~14 km above sea level, asl). The initial phase lasted 27 hours and the tephra fall caused severe disruption over the Argentinean Patagonia (Collini et al. 2013; Schipper et al. 2013; Jay et al. 2014; Murriello and García, 2023) and around PCCV in Chile (e.g., Marin et al., 2020; Vergara-Pinto and Marin, 2023; Vergara-Pinto and Romero, 2023). In the following days, the eruption column oscillated between heights of 3-10 km asl fed by the waning explosive phase (Castro et al. 2013). Lava effusion started on June 15 (Bertin et al. 2015), which was coincident with explosive activity characterized by mixed gas and ash jetting punctuated by Vulcanian blasts with eruption columns up to 6 km high (Schipper et al. 2013). During the eruption, the explosivity correlated directly with the number of earthquakes per hour. Most of the tephra dispersal occurred towards the NNE and ESE as a result of the prevailing winds. The effusive phase had discharge rates up to 70 m^3s^{-1} and finished by mid-2012 (Bertin et al. 2015). The rhyodacitic lava flow covered ~7 km^2 with the extent limited by a graben and the 1960 lava flow to the south. While the 1960 eruption formed a 4 km-length fissure system, the 2011-2012 eruptions were centralized, forming a 0.5 x 0.9 km-diameter pyroclastic cone. Northeast of this cone, proximal tephra fall sequences, and composite PDC-tephra fall-ballistic deposits reached ~3 m and > 15 m-thick, respectively. Since the eruption, at least three ground uplift events have occurred between 2012 and 2019 at rates from 6 to 45 cm/yr, resulting in >1 m total uplift (Euillades et al., 2017; Delgado, 2021).

The 2011-2012 tephra fall deposit was characterized in detail by Pistolesi et al. (2015). The pyroclastic units from the main sub-Plinian phase and the activity up to June 11 correspond to Unit I (layers A to F, deposited by 4-5 June), Unit II (layers G to H, deposited by 5-6 June) and Unit III (layers K1 to K5, deposited by 7-11 June). Within 25 km from the vent, the sequence is dominated by multiple lapilli-bearing fall layers (Units I and II) overlain by cm-thick, light gray, ash-rich fall layers (Unit III). In the most proximal outcrops, along the slopes of the PCCVC, a fourth and younger unit can also be recognized and is represented by very fine-grained, thin (few millimeters to 1-2 cm) white ash related to the eruptive activity continuing to the end of the eruption in 2012.

Table 1. Bulk and dense rock equivalent (DRE) tephra volume estimates for the 2011-2012 Puyehue-Cordón Caulle VEI 4 eruption according to different authors, including the number of field control points (FCPs). Methods include E = exponential thinning (Pyle, 1989; Fierstein and Nathenson, 1992), PL = Power Law (Bonadonna and Houghton, 2005) and W=Weibull (Bonadonna and Costa, 2012).

Reference	Tephra volume estimate (km^3)	Type of estimate	FCPs	Method
Gaitan et al. (2011)	1.46	Bulk	276	Krigging/GIS
Amigo et al. (2012)	0.82 (0.25)	Bulk (DRE)	–	E
Silva et al (2012)	0.5-1.0 (0.2-0.4)	Bulk (DRE)	–	–
Alloway et al. (2015)	1.0	Bulk	400	–
Pistolesi et al. (2015)	0.76-1.26	Bulk	70	E/PL/W
Naranjo et al. (2017)	0.98 (0.39)	Bulk (DRE)	–	E

As shown in Table 1, several authors have estimated the bulk and DRE volume of the tephra fall deposit.

Deposit stratigraphy

The most proximal locations observed E and NE from the vent (~1.2 km) consist of a coarse grained, lapilli-to-bomb sized, pumice tephra fall deposit of ~3 to 3.2 m in overall thickness. These deposits are well bedded and have alternate finer and coarser pumice fall and ash layers. Complex sequences lying NE from the vent reflect the interplay between the coincident tephra fall and pyroclastic density currents during the sustained phase of the eruption.

At medial downwind locations, the tephra fall deposit consists of 3 to 9 pumice lapilli-to-ash layers (Fig. 1). From base to top, the thickest described section (Fig. 1a; 215 highway, 57 cm-thick) starts with layer A consisting of ~7 cm-thick ungraded fine white sub-rounded lapilli pumice; largest-sized pumice fragments are highly vesicular and up to 0.7

cm in diameter. Above, layer B is a ~14 cm-thick non-graded fine-to-medium white pinkish lapilli pumice layer with largest clasts up to 2.5 cm in diameter. Layers A and B contain 5-15% angular black cognate lithics (0.1-0.3 cm diameter). Layers C and D (8 and 5 cm-thick, respectively) are inversely graded and contain fine-to-medium clear-brown to yellowish blocky lapilli pumice. To the top, the sequence has two layers, named E and F, with thicknesses of 4 and 3 cm, respectively; these layers are composed of ungraded, medium yellowish subrounded or blocky lapilli with the largest particles reaching 1.5 and 2.0 cm in diameter. Increasing concentrations of angular black lithics are observed towards the top, some up to 1 cm in diameter. While layer H consists of ~2 cm-thick coarse ash and fine lapilli with a white-grayish color, the package of K layers is ~4 cm-thick and contains fine yellowish lapilli pumice with overall reverse grading. The uppermost layer (L) consists of ~2 cm of finely laminated gray ash. According to the interpretation of Pistolesi et al (2015), layers A-F comprise Unit I, while Unit II are layers G and H. All the layers in K form Unit III, whereas Unit IV corresponds to layer L. The integrity of the so-called Unit I is generally well-preserved in the farthest exposures of the medial sites (Fig. 1b, c), however, layers A and D-F thin out rapidly and the contact between B and C becomes diffuse.

The medial crosswind deposits, north of Puyehue-Cordón Caulle are different from the downwind exposures: the basal layer is a massive coarse brown pumiceous ash (A-F; ~1.5 cm-thick). On top, layer G (~3.0 cm-thick) is composed of reverse-graded fine-to-medium grained white lapilli pumiceous fragments (~50%), black volcanic glass (~40%), and dark angular lithic fragments (~10%) from 0.4 to 1.0 cm diameter. However, this layer has only been found up to 6.5 km N from the vent (Fig. 1d). Above this layer, the Unit III sequence consists of at least five layers (totaling >5 cm), characterized by alternating white fine ash and dark-black glassy angular fragments. To the lower part of the sequence, the contacts are sharp, while towards the top they are mainly gradational.

At distal locations, the downwind tephra fall consists of a single homogeneous white or grayish ash fall layer with some color grading in the middle of the vertical exposure (Fig. 1e, f) with the thickness varying from a few mm to a few cm.

The integrity of the proximal-to-medial sections agrees with the stratigraphy described by Pistolesi et al (2015). Moreover, we did not notice evidence of remobilization or deposit transformation at selected sites for this study. Thus, we suggest all our observations well represent the primary tephra fall deposit and are suitable for volume estimates.

Methods

Our dataset contains 270 proximal to distal tephra FCPs (Supplementary Table S1) of which 221 were collected in the Argentinean Patagonia between June 7 and July 31, 2011, by one of the authors (JJG). Discrete ash resuspension events occurred at least

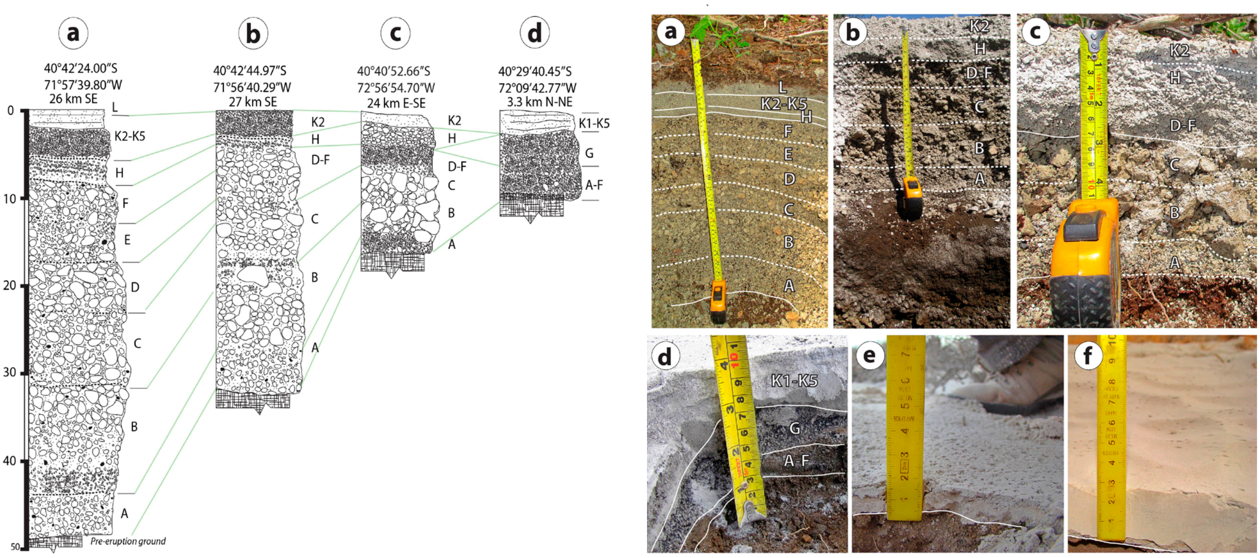

Figure 1.— Stratigraphy, internal architecture, and components of the 2011-2012 eruption tephra fall deposit. The thinning of the sequence is observed along the main dispersal axis (SE; a, and b) but also in the crosswind sections (c and d). Distal deposits lack any observable internal architecture (e and f).

five times between June and July 2011 (Forte et al. 2018). However, the comprehensive remobilization of the distal ash (erosion, transport, and re-deposition) occurred months to years after the initial phase of the eruption and involved a large-scale transformation of the deposit architecture (Dominguez et al. 2020). Our distal sites were in wind-protected areas that showed no evidence of aeolian remobilization or water runoff. The remaining 49 FCPs reported in this work were studied across three periods of fieldwork in Chile and Argentina between June 16 and 20 , 2011, January 5-9 and 25, 2012 by JER and FJS (authors). In these areas, tephra has been removed by hydrologic processes for years after the eruption, affecting watersheds and their corresponding deltas (Beigt et al. 2019). We ensured that the FCP sites were in areas protected from erosion, re-deposition and slope run-off. Another 10 follow-up observations were carried out to validate initial profile descriptions in the proximal-medial zone in January 2018. We compared measurements of tephra thickness at these sites and found that any changes measured were smaller than 4 % of the original thickness. In addition, we carried out stratigraphic descriptions that were compared to published works (e.g., Pistolesi et al., 2015) to verify the preservation of all primary features within the deposits. In summary, we do not expect that our thickness measurements and subsequent volume estimates have been affected by erosive processes, as observed in tephras subject to thickness changes at other volcanoes (see Cutler et al. 2018, 2020).

Figure 1 was obtained using R (R core team, 2021) and shows a directional variogram for the data in different directions (0°, 45°, 90° and 135°). There are no major differences among the different directions (Fig. 2a), suggesting that the data is homogeneously distributed, so the process should be considered as isotropic. Fig. 2b also shows the Voronoi tessellation, where it is evident that the Gaitán et al. (2011a) dataset concentrated in more distant areas from the crater, whereas Romero et al. (2012) and Swanson et al. (2016) made observations in areas closer to the crater. The measurements are also distributed well around the deposition zone but access is limited.

We assign each FCP (thickness value and latitude and longitude) a correlative identifier (IDs between 1 and 270). We then take sub-samples without repositioning of the FCP dataset for different numbers of FCPs where n_i is the number of FCPs (Supplementary Table S2). Increasing in intervals of 10 FCP points, we produce 4 sub-samples for n_i =10 to n_i =50. Then for n_i =60 to n_i =120, we obtain 3 different sub-samples for the value of n_i. For n_i =130 to n_i =180 we generate 2 sub-samples for each value of n. Finally, for n_i =190 to n_i =250, we obtain only one sub-sample per value of n (Supplementary Table S2). This results in 60 subsets of FCPs which we use to construct individual isopach maps (arbitrary contours depending on the dataset; Supplementary Table S2) and the related volume estimate.

All the isopachs were drawn by two volcanologists without any field experience in the deposit or any knowledge of the existing isopach maps, to avoid bias from previous work. However, to help in the “blind” isopach drawing process, they were advised about the location of the vent and the approximate dispersal direction (e.g., towards the E). Each volcanologist used the same dataset to produce 60 isopach maps; they first drew the maps with the smaller n_i datasets. The subjectivity of the scientist during the drawing process is not evaluated in this contribution, its influence in the isopach shape and volume estimate was previously reported in Bernard et al. (2013). We calculate the volumes of the tephra deposit using the AshCalc online tool (Daggit et al., 2014) which is based on the thickness–area relationships to derive a volume as follows:

$$\int_0^\infty T(x)\,dA) = 2\int_0^\infty T(x)\,dx \qquad (1)$$

Where $T(x)$ corresponds to the isopach area. Multiple methods have proposed different relationships between the thickness T and the isopach area. AshCalc allows using the exponential method (eq. 2; Pyle, 1989), the exponential method through the trapezoidal rule for multiple linear segments (Fierstein and Nathenson 1992), the Power Law method (eq. 3; Bonadonna et al., 1998; Bonadonna and Houghton, 2005), and the Weibull method (eq. 4; Bonadonna and Costa 2012).

$$T(x) = ce^{-mx} \qquad (2)$$

$$T(x) = cx^{-m} \qquad (3)$$

$$T(x) = \theta\left(\frac{x}{\lambda}\right)^{k-2} e^{\left(\frac{x}{\lambda}\right)^{k}} \qquad (4)$$

In eq. 2 c is the theoretical maximum thickness at the vent and m the rate of decrease in tephra thickness, whereas in eq. 3 c represents a linear scaling factor.

In eq. 4, λ represents the characteristic decay length scale of deposit thinning (typically expressed in kilometers), θ represents a thickness scale (typically expressed in centimeters), and k is a shape parameter (dimensionless) (Bonadonna and Houghton, 2005). These models require some specific inputs, such as the number of exponential segments to be integrated for the exponential model, or the number of hill-climbing runs, number of iterations per hill-climbing run and upper and lower bounds for λ and k (Daggit et al., 2014). Instructions to determine the latter are provided in the software, and our choice is available in Supplementary Table S3, alongside the full list of the volume estimates. We did not use the Power-Law method because it requires the choice of proximal and distal limits of integration, which requires additional information considered unknown in this "blind-type" exercise (Houghton and Bonadonna 2005).

In order to estimate a minimum sample size to obtain a confident tephra fall volume, we consider a regression model with one break point (Muggeo 2003) in the following way (eq. 5 and 6):

$$Volume_i = \alpha + \beta \times n_i, \text{ for } n_i < \varphi \quad (5)$$

$$Volume_i = \alpha - \varphi \times \gamma + (\beta + \gamma) \times n_i, \text{ for } n_i \geq \varphi \quad (6)$$

Where $Volume_i$ is the estimation based on the exponential or Weibull models for the tephra fall volume for the respective sample size. In other words, the model considers two continuous regression lines with different intercepts and slopes for the intervals where $n_i < \varphi$ and $n_i \geq \varphi$. Two hypotheses are of interest:

$$H_0 : \beta + \gamma = 0, \text{ versus } H_1 : \beta + \gamma \neq 0, \text{ (7), and}$$

$$H_0 : \alpha - \varphi \times \gamma = v_0, \text{ versus } H_1 : \alpha - \varphi \times \gamma \neq v_0 \quad (8)$$

where v_0 is the estimated tephra fall volume, based on the complete data set for the respective model (i.e., v_0=1.214 and v_0=1.103 for the exponential and Weibull models, respectively).

We test two hypotheses; the first indicates that, for any $n_i \geq \varphi$, the estimated volume is constant, and the second hypothesis is valid if such constant is the "true" tephra fall volume for $n_i > \varphi$. If H_0 were validated for (7) and (8), we could say that the estimation of the tephra fall volume based on the sample size n_i is the same (in a statistical sense) as that obtained based on the complete dataset (n_i=270), for $n_i \geq \varphi$. For this reason, the estimation of φ will suggest a sample size for which the tephra fall volume is estimated confidently. We estimate the following using the segmented package (Muggeo 2008) of R software (R Core Team 2021).

To explore the influence of the FCPs and their related volume estimates on the ESPs, we estimate the total erupted mass (M_T, eq. 9), considering the erupted material in layers A-F during c. 27 hours (paroxysmal phase) and the rest of the eruption as layers H-K2 (Bonadonna et al. 2015b; Pistolesi et al. 2015), as follows:

$$\begin{aligned} M_T &= Volume_i \times (f_{A-F} \times d_{A-F} + f_{H-K2} \times d_{H-K2}) \\ &= M_{A-F} + M_{H-K2} \end{aligned} \quad (9)$$

We use f to denote the fraction of erupted volume (75% for layers A-F, and 25% for layers H-K2), and d represents the deposit density (560 kg/m^3 and 600 kg m^{-3} for layers A-F and H-K2, respectively; Bonadonna et al. 2015b; Pistolesi et al. 2015). The peak

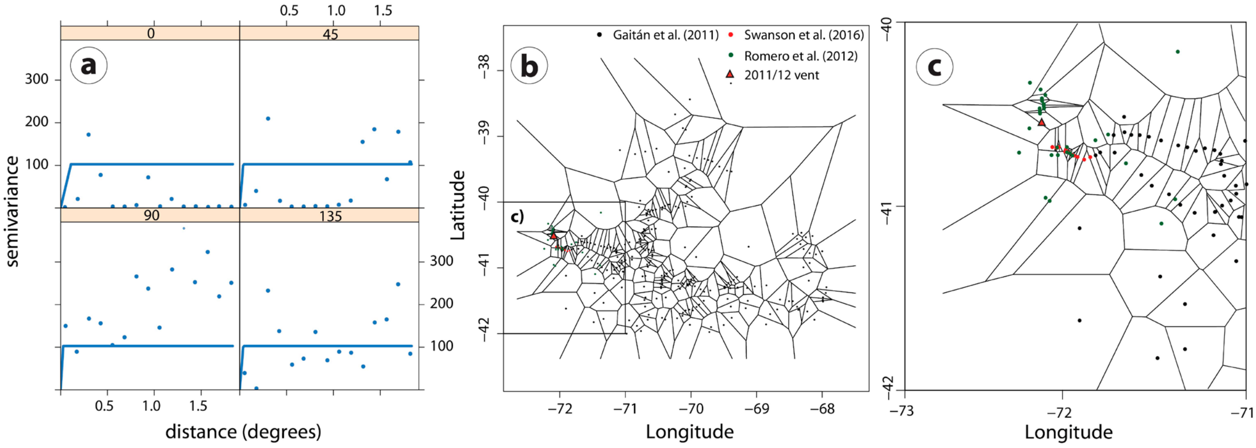

Figure 2.— Directional variogram in the 0°, 45°, 90° and 135° (a) and Voronoi tessellation (b) for the 270 measurements of tephra FCPs of the Puyehue-Cordón Caulle eruption in 2011-2012. (c) is a zoom of the indicated area in (b). These diagrams show that the FCPs are distributed homogeneously rather than in a preferential direction.

mass eruption rate (MER_{A-F}, eq. 10) is estimated as:

$$MER_{A-F} = \left(\frac{M}{t}\right)_{A-F} \quad (10)$$

where t represents the duration (s) of the paroxysmal activity. Therefore, the total magnitude of the eruption (M, eq. 11) and the maximum intensity (I_{A-F}, eq. 12), are obtained following Pyle (2015) as below:

$$M = log_{10}\left(M_T\right) - 7 \quad (11)$$

$$I_{A-F} = log_{10}\left(MER_{A-F}\right) + 3 \quad (12)$$

Finally, the plume top height (H_T, expressed in km above the vent) are obtained using the Matin et al. (2009) equation in function of the MER, as follows:

$$H_T = 0.304 \times MER_{A-F}{}^{0.241} \quad (13)$$

Results

Deposit distribution

The full-dataset isopach map (Fig. 3) shows E-SE distribution of the tephra deposit, mainly over Patagonia Argentina. During the eruption, most of the

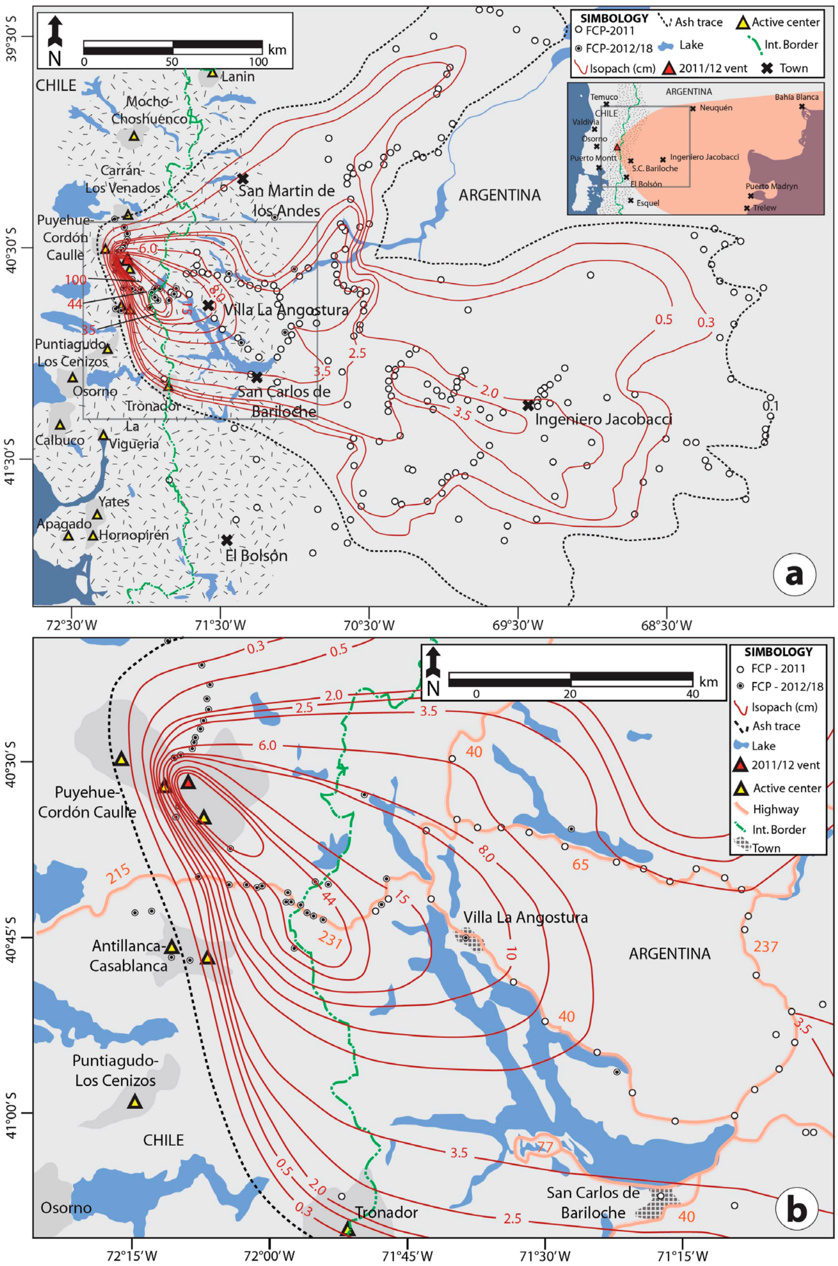

Figure 3.— Consensual total deposit isopach map. a) Overall distribution and b) medial-to-proximal deposit distribution. All the isopachs values are given in cm. In a) the Andes cordillera is indicated with the igneous texture.

Argentinean Pampa and some populated cities such as Neuquén were affected by the distal deposition of ashfall (Fig. 3a). The thinnest measured isopach was 1 mm thick and encompasses nearly 70,000 km^2. Ash traces, fine enough to be transported over longer distances may have fallen in the Atlantic Ocean, thus accounting for a volume difficult to constrain. At intermediate locations (up to ~230 km downwind), the tephra deposit reaches between 2 and 6 cm-thick to the E-SE. That portion of the deposit occupies an area of ~20,000 km^2 and its shape is highly irregular; it develops two main dispersal axes to the NE and E-SE, because of complex high-altitude and surface wind regimes and/or the local influence of topographic features. The thickest isopachs (>6 cm) display regular, ellipsoidal shapes and are distributed obliquely to the 215 and 231 international highways, over the town of Villa La Angostura (Fig. 3b), up to 40 km in the downwind direction. We adopt the nomenclature of Pistolesi et al. (2015) to describe the internal deposit architecture.

Isopach drawing and volume estimates

In all the isopach map iterations, increasing the FCP number in the different datasets yields an increasing number and complexity of isopachs. Isopach maps constructed from only 10 FCPs produces 3 or 4 rough isopachs, in contrast to ≥10 isopachs being drawn when the datasets include ≥110 FCPs (Supplementary Table S4). Increasing the number of FCP points used corresponds to isopachs changing from elliptical to irregularly shaped contour lines (Fig. 4a-e) which are considered more realistic presentations of the natural deposition of the tephra. For example, the isopach map based on the 150 FCP dataset is fairly like that shown in Fig. 2a, which contains the full FCP dataset. On the other hand, the square root area v/s thickness regression illustrates higher variability for smaller FCP datasets, while larger FCP number datasets generally display a more conservative distribution (Fig. 4f). Considering the full dataset as the most realistic (or exact isopach areas), the absolute percent error of the isopach square root areas obtained with smaller datasets range between 1 and 63%, with average errors in the range 20-33 % and mostly concentrated in the distal isopachs (<0.01 m-thick; Fig. 4).

The bulk volume estimates of the full dataset isopach maps are 1.1 and 1.2 km^3 using the Weibull and exponential methods, respectively (Supplementary Table S3). Therefore, our best volume estimate using both methods is 1.15 ± 0.05 km^3. However, important volume differences are found using the variable FCP number dataset. Using the exponential thinning method, the estimated volumes range from 0.91 to 17.66 times the full-dataset volume (1.15 to 22.7 km^3), while the Weibull method results range from 0.75 to 2.89 times (0.96 to 3.56 km^3). The largest estimates were observed only in the 10A dataset (n_i = 10), but they were not considered for further statistical treatment of data as they represent unrealistic estimates and are associated with volume estimate errors ≥250% (Fig. 5).

The exponential and Weibull methods show volume overestimations of ≥30 % for smaller datasets. In the case of the exponential method, overestimation is mostly in datasets with ≤70 FCPs, while with the Weibull method overestimation is consistently observed with ≤50 FCPs. Conversely, underestimating the volume does not occur using exponential thinning. Using the Weibull method, however, does in some cases underestimate the volume relative to the full dataset (i.e., <20 %) typically when the dataset has n_i = 60–100.

For the exponential model, the p-value for the first and second hypotheses of interest are 0.3206 and 0.8867, respectively (Table 2). For the Weibull model, the p-values for the first and second hypothesis of interest are 0.4351 and 0.1923, respectively (Table 2).

Table 2. Estimates and standard errors (SE) for the regression model with one break point for the estimated tephra fall volume based on the exponential and Weibull models.

	exponential		Weibull	
parameter	Estimate	SE	Estimate	SE
α	2.0307	0.1420	2.0882	0.1678
β	–0.0059	0.0027	–0.0134	0.0046
γ	0.0048	0.0029	0.0129	0.0046
ψ	88.2480	30.2680	60.0000	10.5260
	Statistic (p-value)		Statistic (p-value)	
$H_0 : \beta + \gamma = 0$	–1.0022 (0.3206)		–0.7861 (0.4351)	
$H_0 : \alpha - \varphi \times \gamma = v_0$	0.1425 (0.8867)		1.3038 (0.1923)	

Therefore, in both cases we have statistical support to guarantee that, for $n_i \geq \varphi$, both models provide similar results for the estimated tephra fall volume and the complete data. Specifically, the estimate for φ in the exponential case is 88.25 (95 % confidence interval 27.54 -148.96), and for the Weibull case it is 60.00 (95% confidence interval 38.89-81.11). Therefore, the preferred estimation for a sample size that guarantees a confident tephra fall volume is 89 and 60, with several isopachs ranging from 7 to 8 for the exponential and Weibull models, respectively (Table 2). However, if we consider a more conservative point of view (based on the upper limit of the 95 % confidence intervals), the estimated sample sizes are 149 and 82 (resulting in 8-10 isopachs) for the exponential and Weibull models, respectively.

Table 3. Eruption source parameters (ESPs) of the 2011-2012 Puyehue-Cordón Caulle VEI 5 eruption derived from maximum, minimum and average volume estimates obtained in this study, using both exponential and Weibull methods. The equations utilized to estimate these values are detailed in the Methods section. Preferred values are shaded in gray, according to the values obtained using the full dataset.

	Total Mass (MT), kg 10^{11}	
	Exponential	**Weibull**
Maximum	128.0	20.3
Minimum	6.6	5.3
Average	11.1	8.2
	Magnitude (*M*)	
Maximum	6.1	5.3
Minimum	4.8	4.7
Average	5.0	4.9
	Peak MER (kg s-1) x 106	
Maximum	130.0	21.0
Minimum	6.8	5.8
Average	11.0	8.4
	Intensity (*I*)	
Maximum	11.1	10.3
Minimum	9.8	9.7
Average	10.0	9.9
	Column height, km	
Maximum	27.5	17.7
Minimum	13.5	12.8
Average	14.7	14.1
	VEI	
Maximum	6	5
Minimum	5	4
Average	5	5

For datasets containing more than 90 FCPs, using the exponential model we find that the proximal isopachs return average volumes that contribute nearly 36 % to the total volume, medial isopachs represent 52 % and the distal isopachs are only 12 % of the total volume.

Because of the range of volume estimates from the different datasets, we derive a range of eruption source parameters that differ up to one order of magnitude between the maximum and minimum values. For example, the total erupted mass (6.6 – 128.0 × 10^{11} kg) and peak MER (6.8 – 130.0 × 10^6 kg s^{-1}) by the exponential method (Table 3), and similarly the erupted mass (5.3 – 20.3 ×10^{11} kg) and peak MER (5.8 – 21 ×10^6 kg s^{-1}) by the Weibull method (Fig. 6a). The minimum and maximum magnitude and intensity values vary by 1 unit for both volume estimate methods. Accordingly, the estimated column heights for these values are in the range 13.5-27.5 for the exponential method, and 12.8-17.7 for the Weibull method (Fig. 6b). Our best estimates for peak MER, M, I, and HT are 6.8 ± 0.3 x 10^6 kg s^{-1}, 4.82 ± 0.02, 9.85 ± 0.05, and 13.45 ± 0.15 km, respectively, by considering the whole dataset. Comparatively, these values are similar to the minimum values estimated for ESPs reported in Table 3.

Discussion

Mapping and integration strategies

The approach chosen in our contribution aims to minimize bias in constructing isopach maps by limiting the use of knowledge on the eruption and its deposit, by using only the available data to construct the isopachs by hand-drawing knowing the position of the eruptive vent and the approximate dispersal direction (e.g., towards the E). However, this technique has its own flaws. For instance, Yang and Bursik (2013) identified a lack of adherence to the data in drawing isopachs for hand-drawn maps. Another limitation of hand-drawing is the influence of the local knowledge and experience of the geologist drawing the isopach contours, and the assumptions that modify isopach shapes (Engwell et al., 2015). These works have also proposed alternative strategies, such as the use of thickness trends and their separate modeling using segmented linear regression and ordinary kriging (Yang and Bursik, 2013) or the application of spatial statistical methods (Engwell et al., 2015). However, in recent ‘fully statistical’ algorithms for tephra volume estimation, expert judgment is unavoidable in making some choices (e.g., wind-direction, the limit of the tephra fall area, etc.; Rougier et al., 2022). Considering these differences and limitations, we can only compare the resulting volume estimates of both approaches as reported in the literature. For instance, the cubic B-spline curves under tension used by Engwell et al.

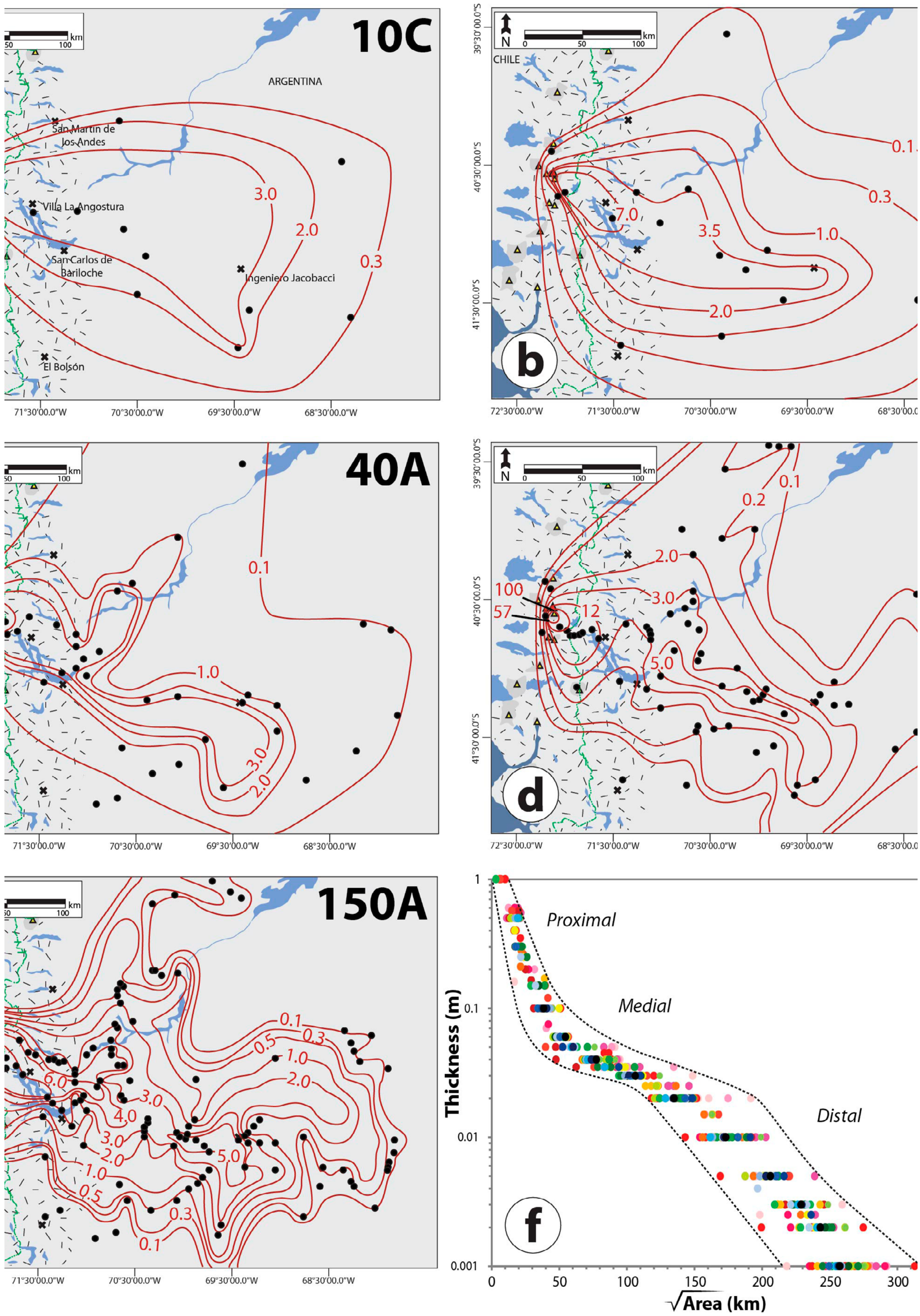

Figure 4.— Examples of isopach maps for randomly selected datasets drawn by two volcanologists. The black bold text in the upper right corner of the plot references the dataset ID where the number indicates the number of FCPs (n_i; see Supplementary Table S4 for details). a)-e) Isopachs produced by increasing the numbers of FCP points. f) Square root of the isopach area versus the isopach thickness. The color of the point indicates the dataset ID. The dashed lines encompass the spread of the isopach area that has been calculated for the same isopach thickness but the different combination of FCP points. The low n_i datasets (hot colours; red, pink and orange) typically occur close to the dashed lines illustrating how using a smaller number of FCPs results in a large range in the isopach area.

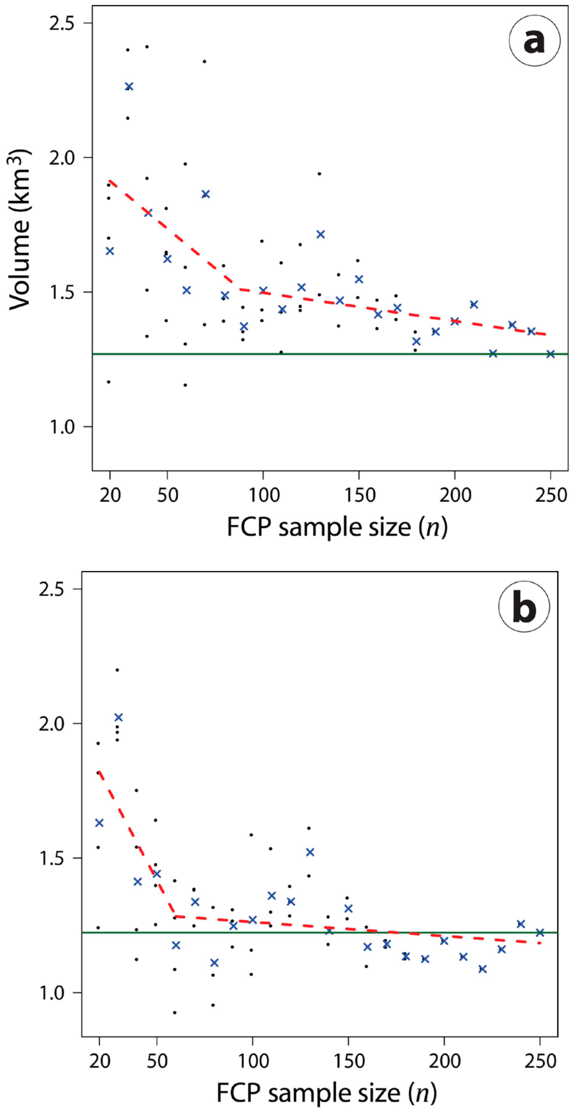

Figure 5.— Estimated tephra fall volume for different sample size (points) and their average (cross) based on the exponential model (a) and Weibull model (b) of the 2011-2012 Puyehue-Cordón Caulle VEI 5 eruption. The red line represents the estimated Volume based on the regression model with one break point and the green line represents the estimated Volume based on the complete data set.

(2015) yield volumes 20-40% smaller compared to hand-drawing isopachs, whereas the method used by Rougier et al. (2022) returned volumes that represent 37-40% of the original bulk tephra estimate by Takarada and Hoshizumi (2020).

Bonadonna et al. (2015a) observed that varying the isopach contouring strategy might result in uncertainty up to 40 % in determining associated erupted volume/mass. In comparison, the different volume integration strategies could result in uncertainties up to 70 %, depending on the deposit exposure, data distribution, and eruption magnitude. From our dataset, we observe uncertainties up to 84 % by comparing the volumes obtained from the exponential thinning and Weibull methods for datasets < 60 FCPs, while the uncertainty is ≤41% for datasets ≥60 FCPs. In addition to these sources of uncertainty, Yang and Jenkins (2023) demonstrate that the misfit between the fitted curves and the isopach data as a result of model uncertainty could affect the tephra volume estimation; they propose that if half or more of the predictions from a certain fitted curve are outside the ±40% range, the curve should not be used for the volume calculation. We do not evaluate model vs. isopach misfit in this contribution.

Field dataset and volume

The volume of the Puyehue-Cordón Caulle 2011-2012 tephra deposit has been studied based on proximal-medial data (0.5-1.0 km^3, e.g., Amigo et al., 2012; Silva et al., 2012; Naranjo et al., 2017), and proximal-to-distal datasets (0.76-1.46 km^3, e.g., Gaitán et al., 2011; Alloway et al., 2015; Pistolesi et al., 2015). The larger volumes estimated from proximal-to-distal data are consistent with the incorporation of larger datasets that include the outer limits of the deposit, and these results agree with our highest-confidence results (1.2-1.3 km^3). This fact is also supported by the datasets and volume estimates in other recent Andean explosive eruptions. For instance, Watt et al. (2009) estimated a volume of 0.17 km^3 for the Chaitén 2008-2009 eruption, mainly based on nine distal isopachs, while Alfano et al. (2011) also incorporated proximal-to-medial data and estimated 0.5-1.0 km^3 utilizing a dozen isopachs. These results demonstrate the importance of considering medial (and proximal) data to constrain tephra volumes more accurately. The Calbuco 2015 tephra fall deposit provides another example. It was mapped in 57 proximal and medial locations by Castruccio et al. (2016), obtaining a range 0.28-0.38 km^3, whereas the proximal-to-distal field observations of Romero et al. (2016) (65 sites) and Van Eaton et al. (2015) (163 sites) provided estimates of 0.27 km^3 and 0.58 ± 0.28 km^3, respectively. Later, Romero et al. (2021) used the full dataset of 150 field points to estimate a proximal-to-distal bulk volume in the 0.25-0.35 km^3 range. All of them applied the Weibull, exponential and Power Law methods. The overall similarity of these estimates, in addition to a good distribution of the field data, agrees with the approximate number of field points required to achieve a 95 % confidence interval using the Weibull

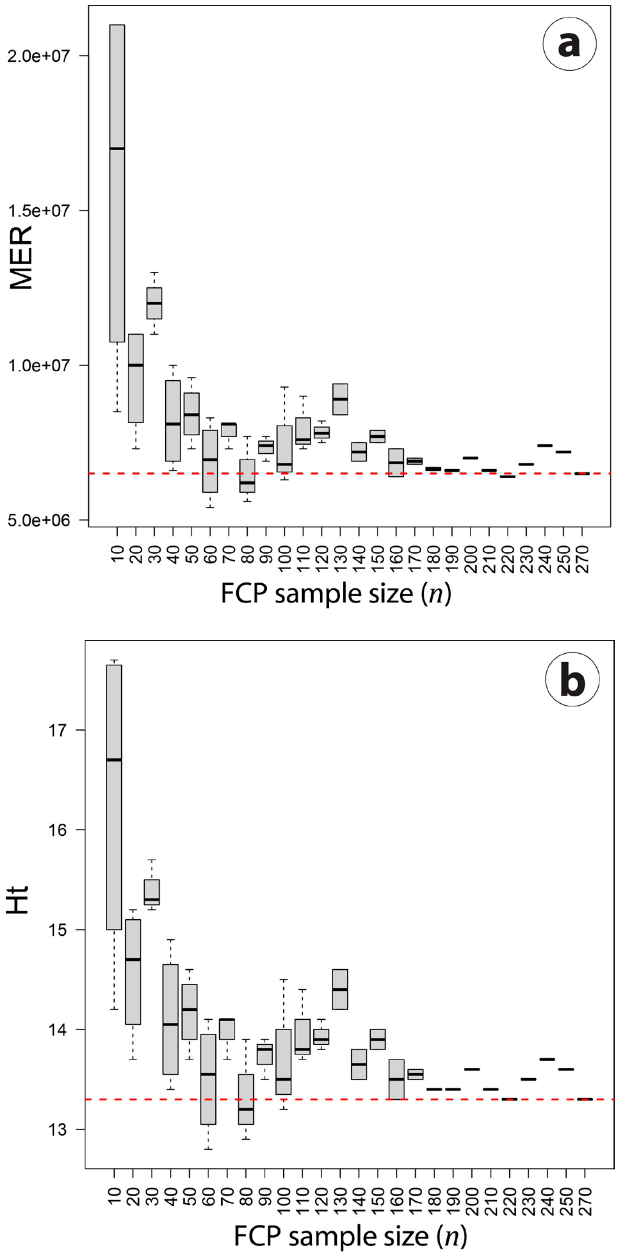

Figure 6.— Box plot of mass eruption rate (MER in kg/s) and column height (Ht in km) carried out using the Weibull model of the 2011-2012 Puyehue-Cordón Caulle VEI 5 eruption. The end of the box (whiskers) indicates minimum and maximum values, while the box length of the box corresponds to the percentiles (the 75th percentile is the upper end, the 25th percentile the lower end, and the middle line is the 50th percentile).

method, as in this contribution. A remarkable example of high-resolution tephra mapping is observed for the Plinian eruption of Hudson volcano in 1991; Banks and Iven (1991) mapped a dozen proximal-to-distal isopachs and estimated a bulk volume of 4 km^3, which does not differ considerably from Scasso et al. (1994) 4.35 km^3 estimate, using fifteen isopachs and 200 field points.

Our results support findings from previous incompletely sampled tephra deposits that similarly found different sub-samples of the field data translates into uncertainties in erupted volume estimates, irrespective of eruption size (e.g., Andronico et al., 2014; Engwell et al., 2015; Buckland et al., 2020). Our exercise of the Puyehue-Cordón-Caulle 2011-2012 tephra fall deposit is a good example on the control of field points on accurately estimating tephra volumes and confirms previous evidence from Engwell et al. (2015), indicating that maps with < 60 points produce volume errors generally > 50 %. Accordingly, small variations in the volume estimate are found at datasets >80-100 points. It is worth mentioning that Engwell et al. (2015) used a range of eruptions with published volumes from 0.003 to 8.2 km^3 and a different isopach drawing method (cubic B-spline curves under tension). Also, because of the extensive thickness data available in our contribution, we have shown that integrating medial FCPs contributes to the largest portion of the total deposit volume (> 50%), thus incompletely sampling deposits at medial areas will produce a larger uncertainty.

Considerations for further studies

The careful investigation of tephra fall deposits with large field datasets provides the best means of determining accurate estimates of tephra volume, mass eruption rates, and interpretations of eruption dynamics. We determined that varying the number (n_i) of FCPs, and consequently the supporting data for isopach drawing, may translate into order of magnitude ranges in the total mass and MER for 2011-2012 PCCVC eruption. Thus, we suggest authors be cautious when determining these parameters with limited FCPs. However, using field data collected at fewer locations can still be informative (Green et al. 2016), but has to consider huge uncertainties, sometimes greater than the volume estimate itself.

In light of our results and accordingly to the available literature, we suggest that tephra fall field mapping considers the total extent of the deposit: 1) if possible, covering from proximal to distal areas, but focusing on the proper characterization of proximal and medial areas as they account most of the erupted volume; 2) distributing FCPs isotropically, avoiding concentrating points along the crosswind or downwind axis only, which will probably result into a forced ellipsoidal distribution; 3) collecting, if possible, at least 60 to 90 field control points with these conditions, allowing the integration of 7-8 isopachs, and 4) estimating erupted volumes as a range, instead of absolute values (e.g., Constantinescu et al. 2022b). In this respect, we consider the best result is represented by the volume estimate derived from the integration of the largest number of FCPs. However, this choice is open to discussion and may depend on a series of physical and statistical considerations that we are not deciphering in detail. Considering the calculation of an exact volume is an unrealistic task, volcanologists are invited to provide a range of results considering different methods, and to report and discuss the different uncertainties that modify these results (e.g., Engwell et al. 2013; Bonadonna et al. 2015a; Biass et al. 2019). This is important as absolute estimates may represent a minimum or maximum, leading to underestimation or overestimation of ESPs, hazard mapping, or numerical modeling (e.g., Constantinescu et al. 2022b).

Conclusions

Studying the tephra fall deposit of the 2011-2012 Puyehue-Cordón Caulle VEI 5 eruption through a high-resolution dataset resulted in a proper estimate of its total volume. However, the results depend on the number of field control points (FCPs). Producing randomly selected sub-datasets of FCPs ranging from 10 to 250 allowed isopach drawing and volume integration through the exponential and Weibull methods. Volume overestimations of $\geq 30\%$ were observed in smaller datasets (i.e., ≤ 70 and ≤ 50 FCPs for the exponential and Weibull methods, respectively). Datasets with 10 points provided 2.9 to 17.7 times the full-dataset volume. Therefore, the preferred estimation for a sample size that guarantees a confident tephra fall volume is 89 and 60 (95 % confidence interval) for the exponential and Weibull methods, to produce 7-8 isopachs. These numbers consider a homogeneous and isotropic distribution of these points, as proximal but especially medial measurements represent a higher proportion of the total deposit volume (36 and 52 %, respectively) to be evaluated. Our best estimates for deposit volume returns a range of 1.15 ± 0.05 km^3 and the overall eruption magnitude of 4.82 ± 0.02 (not considering lava effusion). For the paroxysmal sub-Plinian phase of the eruption, a peak mass eruption rate is estimated at $6.8 \pm 0.3 \times 10^6$ kg s^{-1}, the intensity at 9.85 ± 0.05, and the column height is 13.45 ± 0.15 km. Finally, the deposit-based eruption source parameters are sensitive to tephra volume/mass estimates, as the minimum and maximum total erupted masses may vary by one order of magnitude, thus influencing estimates of mass discharge rate, magnitude, and intensity of the eruption.

DATA AVAILABILITY

The authors declare that all the relevant data supporting the findings of this study are included in the paper, in the Supplementary Tables, available for download in the online version of this article. All other files of interest for readers will be supplied under request.

ACKNOWLEDGEMENTS

We thank E. Cárdenas, C. Pérez, H. Moyano, J. Romero A., M. González, and A. Lara for their support during the fieldwork. Julia Jones provided fruitful discussions and field assistance, while S. Engwell made valuable suggestions on an earlier version of this manuscript. Photos provided by D. Spatafore, I. Silva and P. Forte were helpful for figure design.

DECLARATION OF COMPETING INTEREST

The authors of this article declare that they have no financial, professional or personal conflicts of interest that could have inappropriately influenced this work.

FUNDING

This work was partially supported by US National Science Foundation grants 0823380 and 0917697, the US Forest Service Pacific Northwest Research Station, Dirección de Investigación y Desarrollo (DID), Universidad Austral de Chile, and Center for Climate and Resilience Research (CR)2 (CONICYT/FONDAP/15110009). JER is funded by Fondecyt Iniciación 11241126.

CRediT AUTHORSHIP

Jorge Romero: Conceptualization, Data curation, Formal Analysis, Investigation, Methodology, Supervision, Validation, Writing – original draft, Writing – review & editing. **Diego Gallardo**: Data curation, Formal Analysis, Methodology, Writing – original draft. **Juan Gaitán**: Data curation, Formal Analysis. **Frederick Swanson**: Writing – original draft, Formal Analysis. **Florencia Sánchez**: Formal Analysis. **Marcela Saavedra**: Formal Analysis. **Nikolas Zambrano**: Formal Analysis. **Hannah Buckland**: Methodology, Validation, Writing – original draft, Writing – review & editing. **Inés Rodríguez**: Supervision, Validation, Writing – review & editing.

References

Alfano, F., Bonadonna, C., Volentik, A. C., Connor, C. B., Watt, S. F., Pyle, D. M., & Connor, L. J. (2011). Tephra stratigraphy and eruptive volume of the May, 2008, Chaitén eruption, Chile. *Bulletin of Volcanology*, 73, 613-630. https://doi.org/10.1007/s00445-010-0428-x

Alloway, B. V., Pearce, N. J., Moreno, P. I., Villarosa, G., Jara, I. A., Henríquez, C. A., Sagredo, E. A., Ryan, M. T., & Outes, V. (2022). Refinement of the tephrostratigraphy straddling the northern Patagonian Andes (40-41° S): new tephra markers, reconciling different archives and ascertaining the timing of piedmont deglaciation. *Journal of Quaternary Science*, 37(3), 441-477. https://doi.org/10.1002/jqs.3389

Alloway, B. V., Pearce, N. J. G., Villarosa, G., Outes, V., & Moreno, P. I. (2015). Multiple melt bodies fed the AD 2011 eruption of Puyehue-Cordón Caulle, Chile. *Scientific Reports*, 5(1), 17589. https://doi.org/10.1038/srep17589

Amigo, A., Bertin, D., Orozco, G., Silva, C., & Lara, L. (2012). Pronósticos de dispersión piroclástica y depósitos de caída durante la erupción del Cordón Caulle, junio 2011. In *Actas 13 Congreso Geológico Chileno* (pp. 474-476).

Andronico, D., Scollo, S., Cristaldi, A., & Lo Castro, M. D. (2014). Representivity of incompletely sampled fall deposits in estimating eruption source parameters: a test using the 12-13 January 2011 lava fountain deposit from Mt. Etna volcano, Italy. *Bulletin of volcanology*, 76, 1-14. https://doi.org/10.1007/s00445-014-0861-3

Banks, N.G., & Iven, M. (1991). Report of the United Nations Mission to Volcfin Hudson, Chile, 20 August-15 September 1991. US Geological Survey, Cascades Volcano Observatory.

Basualto, D., Tassara, A., Lazo-Gil, J., Franco-Marin, L., Cardona, C., San Martín, J., Gil-Cruz, F., Calabi-Floddy, M., & Farías, C. (2023). Anatomy of a high-silica eruption as observed by a local seismic network: the June 2011 Puyehue-Cordón Caulle event (southern Andes, Chile), *Solid Earth*, 14, 69-87, https://doi.org/10.5194/se-14-69-2023 https://doi.org/10.5194/se-14-69-2023

Beigt, D; Villarosa, G., Outes, V., Gómez, E.A., & Toyos, G. (2019). Remobilized Cordón Caulle 2011 tephra deposits in north-Patagonian watersheds: Resedimentation at deltaic environments and its implications. *Geomorphology*, 341, 140-152. https://doi.org/10.1016/j.geomorph.2019.05.023

Bernard, B; Bustillos, J., Wade, B., & Hidalgo, S. (2013). Influence of the wind direction variability on the quantification of tephra fallouts: December 2012 and March 2013 Tungurahua eruptions. *Avances*, 5(1), A14-A21. https://doi.org/10.18272/aci.v5i1.112

Bertin, D., Lara, L. E., Basualto, D., Amigo, Á., Cardona, C., Franco, L., Gil, F., & Lazo, J. (2015). High effusion rates of the Cordón Caulle 2011-2012 eruption (Southern Andes) and their relation with the quasi-harmonic tremor. *Geophysical Research Letters*, 42(17), 7054-7063. https://doi.org/10.1002/2015GL064624

Biass, S., Bonadonna, C., & Houghton, B.F. (2019). A step-by-step evaluation of empirical methods to quantify eruption source parameters from tephra-fall deposits. *Journal of Applied Volcanology*, 8(1), 1-16. https://doi.org/10.1186/s13617-018-0081-1

Bonadonna, C., & Houghton, B.F. (2005). Total grain-size distribution and volume of tephra-fall deposits. *Bulletin of Volcanology*, 67, 441-456. 10.1007/s00445-004-0386-2 https://doi.org/10.1007/s00445-004-0386-2

Bonadonna, C., Ernst, G., & Sparks, R. (1998). Thickness variations and volume estimates of tephra fall deposits: the importance of particle Reynolds number. Jou*rnal of Volcanology and Geothermal Research*, 81, 173-187. 10.1016/S0377-0273(98)00007-9 https://doi.org/10.1016/S0377-0273(98)00007-9

Bonadonna, C., Biass, S., & Costa, A. (2015a). Physical characterization of explosive volcanic eruptions based on tephra deposits: propagation of uncertainties and sensitivity analysis. *Journal of Volcanology and Geothermal Research*, 296, 80-100. https://doi.org/10.1016/j.jvolgeores.2015.03.009

Bonadonna, C., Pistolesi, M., Biass, S., Voloschina, M., Romero, J., Coppola, D., Cappola, D., Folch, A., D'Auria, L., Martín-Lorenzo, A., Domínguez, L., Pastore, C., Reyes-Hardy, & M. P., Rodríguez, F. (2022). Physical Characterization of Long-Lasting Hybrid Eruptions: The 2021 Tajogaite Eruption of Cumbre Vieja (La Palma, Canary Islands). *Journal of Geophysical Research: Solid Earth*, 127(11), e2022JB025302. https://doi.org/10.1029/2022JB025302

Bonadonna, C., Pistolesi, M., Cioni, R., Degruyter, W., Elissondo, M., & Baumann, V. (2015). Dynamics of wind-affected volcanic plumes: The example of the 2011 Cordón Caulle eruption, Chile. *Journal of Geophysical Research: Solid Earth*, 120(4), 2242-2261. https://doi.org/10.1002/2014JB011478

Bonadonna, C., & Costa, A. (2012). Estimating the volume of tephra deposits: a new simple strategy. *Geology*, 40(5), 415-418. https://doi.org/10.1130/G32769.1

Bonadonna, C., & Houghton, B.F. (2005). Total grain-size distribution and volume of tephra-fall deposits. *Bulletin of Volcanology*, 67(5), 441-456. https://doi.org/10.1007/s00445-004-0386-2

Buckland, H. M., Cashman, K. V., Engwell, S. L., & Rust, A. C. (2020). Sources of uncertainty in the Mazama isopachs and the implications for interpreting distal tephra deposits from large magnitude eruptions. *Bulletin of Volcanology*, 82, 23 (2020). https://doi.org/10.1007/s00445-020-1362-1

Castro, J. M., Schipper, C. I., Mueller, S. P., Militzer, A. S., Amigo, A., Parejas, C. S., & Jacob, D. (2013). Storage and eruption of near-liquidus rhyolite magma at Cordón Caulle, Chile. *Bulletin of Volcanology*, 75, 1-17. https://doi.org/10.1007/s00445-013-0702-9

Castruccio, A., Clavero, J., Segura, A., Samaniego, P., Roche, O., Le Pennec, J. L., & Droguett, B. (2016). Eruptive parameters and dynamics of the April 2015 sub-Plinian eruptions of Calbuco volcano (southern Chile). *Bulletin of Volcanology*, 78, 1-19. https://doi.org/10.1007/s00445-016-1058-8

Chapron, E., Ariztegui, D., Mulsow, S., Villarosa, G., Pino, M., Outes, V., Juvignié, E., & Crivelli, E. (2006). Impact of the 1960 major subduction earthquake in Northern Patagonia (Chile, Argentina). *Quaternary International*, 158(1), 58-71. https://doi.org/10.1016/j.quaint.2006.05.017

Collini, E., Osores, M.S., Folch, A., Viramonte, J.G., Villarosa, G., & Salmuni, G. (2013). Volcanic ash forecast during the June 2011 Cordón Caulle eruption. *Natural hazards*, 66(2), 389-412. https://doi.org/10.1007/s11069-012-0492-y

Constantinescu, R., White, J. T., Connor, C., Cole, P., Fontijn, K., Barclay, J., & Robertson, R. (2022a). Estimation of eruption source parameters for the 2021 La Soufrière eruption (St. Vincent): implications for quantification of eruption magnitude on volcanic islands. *Geological Society, London, Special Publications*, 539, 107-120. https://doi.org/10.1144/SP539-2023-38

Constantinescu, R., White, J. T., Connor, C. B., Hopulele-Gligor, A., Charbonnier, S., Thouret, J. C., Lindsay, J. M., & Bertin, D. (2022b). Uncertainty quantification of eruption source parameters estimated from tephra fall deposits. *Geophysical Research Letters*, 49(6), e2021GL097425. https://doi.org/10.1029/2021GL097425

Cutler, N.A., Streeter, R.T., Engwell, S.L., Bolton, M.S., Jensen, B.J.L., & Dugmore, A.J. (2020). How does tephra deposit thickness change over time? A calibration exercise based on the 1980 Mount St Helens tephra deposit. *Journal of Volcanology and Geothermal Research*, 399, 106883. https://doi.org/10.1016/j.jvolgeores.2020.106883

Cutler, N.A., Streeter, R.T., Marple, J., Shotter, L.R., Yeoh, J.S., & Dugmore, A.J. (2018). Tephra transformations: variable preservation of tephra layers from two well-studied eruptions. *Bulletin of Volcanology*, 80(11), 1-15. https://doi.org/10.1007/s00445-018-1251-z

Daggitt, M.L., Mather, T.A., Pyle, D.M., & Page, S. (2014). AshCalc-a new tool for the comparison of the exponential, power-law and Weibull models of tephra deposition. *Journal of Applied Volcanology*, 3, 7. https://doi.org/10.1186/2191-5040-3-7

Del Bello, E., Taddeucci, J., Merrison, J. P., Rasmussen, K. R., Andronico, D., Ricci, T., Scarlatto, P., & Iversen, J. J. (2021). Field-based measurements of volcanic ash resuspension by wind. *Earth and Planetary Science Letters*, 554, 116684. https://doi.org/10.1016/j.epsl.2020.116684

Delgado, F. (2021). Rhyolitic volcano dynamics in the Southern Andes: Contributions from 17 years of InSAR observations at Cordón Caulle volcano from 2003 to 2020. *Journal of South American Earth Sciences*, 106, 102841. https://doi.org/10.1016/j.jsames.2020.102841

Domínguez, L., Bonadonna, C., Forte, P., Jarvis, P.A., Cioni, R., Mingari, L., Bran, D., & Panebianco, J.E. (2020). Aeolian Remobilisation of the 2011-Cordón Caulle Tephra-Fallout Deposit: Example of an Important Process in the Life Cycle of Volcanic Ash. *Frontiers in*

Earth Science, 7, 343. https://doi.org/10.3389/feart.2019.00343

Domínguez, L., Bonadonna, C., Frischknecht, C., Menoni, S., & García, A. (2021). Integrative Post-event Impact Assessment Framework for Volcanic Eruptions: A Disaster Forensic Investigation of the 2011-2012 Eruption of the Cordón Caulle Volcano (Chile). *Frontiers in Earth Science*, 9, 645945. https://doi.org/10.3389/feart.2021.645945

Elissondo, M., Baumann, V., Bonadonna, C., Pistolesi, M., Cioni, R., Bertagnini, A., Biass, S., Herrero, J-C., & González, R. (2016). Chronology and impact of the 2011 Cordon Caulle eruption, Chile. *Natural Hazards and Earth System Sciences*, 16, 675-704. https://doi.org/10.5194/nhess-16-675-2016

Engwell, S. L., Sparks, R. S. J., & Aspinall, W. P. (2013). Quantifying uncertainties in the measurement of tephra fall thickness. *Journal of Applied Volcanology*, 2(1), 5. https://doi.org/10.1186/2191-5040-2-5

Engwell, S. L., Aspinall, W. P., & Sparks, R. S. J. (2015). An objective method for the production of isopach maps and implications for the estimation of tephra deposit volumes and their uncertainties. *Bulletin of Volcanology*, 77, 61 (2015). https://doi.org/10.1007/s00445-015-0942-y

Euillades, P. A., Euillades, L. D., Blanco, M. H., Velez, M. L., Grosse, P., & Sosa, G. J. (2017). Co-eruptive subsidence and post-eruptive uplift associated with the 2011-2012 eruption of Puyehue-Cordón Caulle, Chile, revealed by DInSAR. *Journal of Volcanology and Geothermal Research*, 344, 257-269. https://doi.org/10.1016/j.jvolgeores.2017.06.023

Fierstein, J., & Nathenson, M. (1992). Another look at the calculation of fallout tephra volumes. *Bulletin of Volcanology*, 54(2), 156-167. https://doi.org/10.1007/BF00278005

Gaitán, J. J., Ayesa, J. A., Umaña, F., Raffo, F., Bran, D. B., & de Bariloche, E. S. (2011a). *Cartografía del área afectada por cenizas volcánicas en las provincias de Río Negro y Neuquén*. INTA Bariloche, Argentina. http://dx.doi.org/10.13140/2.1.2059.4881

Gaitán, J. J., Bran, D. B., Marciani, S., Umaña, F., Ayesa, J. A., & Raffo, F. (2011b). *Monitoreo de la vegetación en áreas afectadas por cenizas volcánicas en Río Negro y Neuquén*. INTA Bariloche, Argentina. http://dx.doi.org/10.13140/2.1.3894.4964

Gerlach, D. C., Frey, F. A., Moreno-Roa, H., & López-Escobar, L. (1988). Recent volcanism in the Puyehue-Cordon Caulle region, Southern Andes, Chile (40· 5° S): petrogenesis of evolved lavas. *Journal of Petrology* 29(2), 333-382. https://doi.org/10.1093/petrology/29.2.333

Green, R. M., Bebbington, M. S., Jones, G., Cronin, S. J., & Turner, M. B. (2016). Estimation of tephra volumes from sparse and incompletely observed deposit thicknesses. *Bulletin of Volcanology*, 78(4), 25. https://doi.org/10.1007/s00445-016-1016-5

Hickey, R. L., Frey, F.A., & Gerlach, D.C. (1986). Multiple sources for basaltic arc rocks from the southern volcanic zone of the Andes (34-41 S): trace element and isotopic evidence for contributions from subducted oceanic crust, mantle, and continental crust. *Journal of Geophysical Research: Solid Earth*, 91(B6), 5963-5983. https://doi.org/10.1029/JB091iB06p05963

Jay, J., Costa, F., Pritchard, M., Lara, L., Singer, B., & Herrin, J. (2014). Locating magma reservoirs using InSAR and petrology before and during the 2011-2012 Cordón Caulle silicic eruption. *Earth and Planetary Science Letters*, 395, 254-266. https://doi.org/10.1016/j.epsl.2014.03.046

Katsui, Y., & Katz, H. R. (1967). Lateral fissure eruptions in the southern Andes of Chile. *Journal of the Faculty of Science, Hokkaido University, Geology and Mineralogy*, 13(4), 433-448.

Klawonn, M., Houghton, B. F., Swanson, D. A., Fagents, S. A., Wessel, P., & Wolfe, C. J. (2014). From field data to volumes: constraining uncertainties in pyroclastic eruption parameters. *Bulletin of Volcanology*, 76(7), 839. https://doi.org/10.1007/s00445-014-0839-1

Krumm, F. (1923). Topographische und geologische Nachrichten über die Gegend stlich des Ranco Sees in Süd Chile, im Besonderen über den jüngsten Vulkanausbruch 'Los Azufres' (Dezember 1921). *Geologische Rundschau*, 14, 146-150 https://doi.org/10.1007/BF01769035

Lara, L., Amigo, A., Silva, C., Orozco, G., & Bertin, D. (2012). La erupción 2011-2012 del Cordón Caulle: antecedentes generales y rasgos notables de una erupción en curso. In *Actas XIII Congreso Geológico Chileno* (pp. 531-533).

Lara, L. E., Lavenu, A., Cembrano, J., & Rodríguez, C. (2006a). Structural controls of volcanism in transversal chains: resheared faults and neotectonics in the Cordón Caulle-Puyehue area (40.5 S), Southern Andes. *Journal of Volcanology and Geothermal Research*, 158(1-2), 70-86. https://doi.org/10.1016/j.jvolgeores.2006.04.017

Lara, L. E., & Moreno, H. (2006). *Geología del Complejo Volcánico Puyehue-Cordón Caulle, X Región de Los Lagos*. Carta Geológica de Chile: Serie Geología Básica 99, Servicio Nacional de Geología y Minería de Chile.

Lara, L. E., Moreno, H., Naranjo, J. A., Matthews, S., & De Arce, C. P. (2006). Magmatic evolution of the Puyehue-Cordón Caulle Volcanic Complex (40 S), Southern Andean Volcanic Zone: from shield to unusual rhyolitic fissure volcanism. *Journal of Volcanology and Geothermal Research*, 157(4), 343-366. https://doi.org/10.1016/j.jvolgeores.2006.04.010

Lara, L. E., Naranjo, J. A., & Moreno, H. (2004). Rhyodacitic fissure eruption in Southern Andes (Cordón Caulle; 40.5 S) after the 1960 (Mw: 9.5) Chilean earthquake: a structural interpretation. *Journal of Volcanology and Geothermal Research*, 138(1-2), 127-138. https://doi.org/10.1016/j.jvolgeores.2004.06.009

López-Escobar, L., Vergara, M., & Frey, F. A. (1981). Petrology and geochemistry of lavas from Antuco Volcano, a basaltic volcano of the Southern Andes (37°25′S): *Journal of Volcanology and Geothermal Research*, 11, 329-352. https://doi.org/10.1016/0377-0273(81)90030-5

Marin, A., Vergara-Pinto, F., Prado, F., & Farias, C. (2020). Living near volcanoes: Scoping the gaps between the local community and volcanic experts in southern Chile. *Journal of Volcanology and Geothermal Research*, 398, 106903. https://doi.org/10.1016/j.jvolgeores.2020.106903

Mastin, L. G., Guffanti, M., Servranckx, R., Webley, P., Barsotti, S., Dean, K., Durant, A., Ewert, J.W., Neri, A., Rose, W.I., Schneider, D., Siebert, L., Stunder, B., Swanson, G., Tupper, A., Volentik, A., & Waythomas, C. F. (2009). A multidisciplinary effort to assign realistic source parameters to models of volcanic ash-cloud transport and dispersion during eruptions. *Journal of Volcanology and Geothermal Research*, 186(1-2), 10-21. https://doi.org/10.1016/j.jvolgeores.2009.01.008

Montiel, M., González, M. E., Christie, D. A., Muñoz, A. A., & Crisafulli, C. M. (2022). Direct effects of tephra fallout from the Puyehue-Cordón Caulle Volcanic Complex on Nothofagus pumilio ring widths in northern Patagonia. *Dendrochronologia*, 75, 125998. https://doi.org/10.1016/j.dendro.2022.125998

Muggeo, V. R. M. (2003). Estimating regression models with unknown break-points. *Statistics in Medicine*, 22, 3055-3071. https://doi.org/10.1002/sim.1545

Muggeo, V. R. M. (2008). Segmented: an R Package to Fit Regression Models with Broken-Line Relationships. *R News*, 8/1, 20-25.

Murriello, S., & García, G. B. (Eds.). (2023). *A diez años de la erupción del Puyehue-Cordón Caulle*. Editorial UNRN. https://doi.org/10.4000/books.eunrn.19938

Naranjo, J. A., Singer, B. S., Jicha, B. R., Moreno, H., & Lara, L. E. (2017). Holocene tephra succession of Puyehue-Cordón Caulle and Antillanca/Casablanca volcanic complexes, southern Andes (40-41 S). *Journal of Volcanology and Geothermal Research*, 332, 109-128. https://doi.org/10.1016/j.jvolgeores.2016.11.017

Newhall, C. G., & Self, S. (1982). The volcanic explosivity index (VEI) an estimate of explosive magnitude for historical volcanism. *Journal of Geophysical Research: Oceans*, 87(C2): 1231-1238. https://doi.org/10.1029/JC087iC02p01231

Pistolesi, M., Cioni, R., Bonadonna, C., Elissondo, M., Baumann, V., Bertagnini, A., Chiari, L., González, R., Rosi, M., & Francalanci, L. (2015). Complex dynamics of small-moderate volcanic events: the example of the 2011 rhyolitic Cordón Caulle eruption, Chile. *Bulletin of Volcanology*, 77(1), 3. https://doi.org/10.1007/s00445-014-0898-3

Primerano, P., Giordano, G., Costa, A., de Vita, S., & Di Vito, M. A. (2021). Reconstructing fallout features and dispersal of Cretaio Tephra (Ischia Island, Italy) through field data analysis and numerical modelling: Implications for hazard assessment. *Journal of Volcanology and Geothermal Research*, 415, 107248. https://doi.org/10.1016/j.jvolgeores.2021.107248

Pyle, D. M. (2015). Sizes of volcanic eruptions. In B. Houghton, S. McNutt, H. Rymer & J. Stix (Eds.), *The encyclopedia of volcanoes* (pp. 257-264). Elsevier. https://doi.org/10.1016/B978-0-12-385938-9.00013-4

Pyle, D. M. (1989). The thickness, volume and grainsize of tephra fall deposits. *Bulletin of*

Volcanology, 51(1), 1-15. https://doi.org/10.1007/BF01086757

R Core Team (2021). *R: A language and environment for statistical computing*. R Foundation for Statistical Computing, Vienna, Austria. https://www.R-project.org/.

Romero, J.E., Morgavi, D., Arzilli, F., Daga, R., Caselli, A., Reckziegel, F., Viramonte, J., Díaz-Alvarado, J., Polacci, M., Burton, M., & Perugini, D. (2016). Eruption dynamics of the 22-23 April 2015 Calbuco Volcano (southern Chile): Analyses of tephra fall deposits. *Journal of Volcanology and Geothermal Research*, 317, 15-29. https://doi.org/10.1016/j.jvolgeores.2016.02.027

Romero, J. E., Alloway, B. V., Gutiérrez, R., Bertín, D., Castruccio, A., Villarosa, G., Schipper, I. C., Guevara, A., Bustillos, J., Pisello, A., Daga, R., Montiel, M., Gleeman, E., González, M., Morgavi, D., Ribeiro Guevara, S., & Mella, M. (2021). Centennial-scale eruptive diversity at Volcán Calbuco (41.3° S; Northwest Patagonia) deduced from historic tephra cover-bed and dendrochronologic archives. *Journal of Volcanology and Geothermal Research*, 107281. https://doi.org/10.1016/j.jvolgeores.2021.107281

Romero, J.E., Vergara-Pinto, F., Forte, P., Ovalle, J. & Sánchez, F. (2024). The Andean Southern Volcanic Zone: a review on the legacy of the latest volcanic eruptions. Andean Geology, 51 (2), 379-412. https://doi.org/10.5027/andgeoV51n2-3681

Rougier, J. C., Sparks, R. S. J., Aspinall, W. P., & Mahony, S. H. (2022). Estimating tephra fall volume from point-referenced thickness measurements. *Geophysical Journal International*, 230(3), 1699-1710. https://doi.org/10.1093/gji/ggac131

Scasso, R. A., Corbella, H., & Tiberi, P. (1994). Sedimentological analysis of the tephra from the 12-15 August 1991 eruption of Hudson volcano. *Bulletin of Volcanology*, 56, 121-132. https://doi.org/10.1007/s004450050021

Schipper, C. I., Castro, J. M., Tuffen, H., James, M. R., & How, P. (2013). Shallow vent architecture during hybrid explosive-effusive activity at Cordón Caulle (Chile, 2011-12): evidence from direct observations and pyroclast textures. *Journal of Volcanology and Geothermal Research*, 262, 25-37. https://doi.org/10.1016/j.jvolgeores.2013.06.005

Sepúlveda, F., Lahsen, A., Bonvalot, S., Cembrano, J., Alvarado, A., & Letelier, P. (2005). Morpho-structural evolution of the Cordón Caulle geothermal region, Southern Volcanic Zone, Chile: Insights from gravity and 40Ar/39Ar dating. *Journal of Volcanology and Geothermal Research*, 148(1-2), 165-189. https://doi.org/10.1016/j.jvolgeores.2005.03.020

Seropian, G., Schipper, C. I., Harmon, L. J., Smithies, S. L., Kennedy, B. M., Castro, J. M., Alloway, B., & Forte, P. (2021). A century of ongoing silicic volcanism at Cordón Caulle, Chile: New constraints on the magmatic system involved in the 1921-1922, 1960 and 2011-2012 eruptions. *Journal of Volcanology and Geothermal Research*, 420, 107406. https://doi.org/10.1016/j.jvolgeores.2021.107406

Silva, C., Lara, L., Amigo, A., Bertin, D., & Orozco, G. (2012). Caracterización de los principales productos eruptivos emitidos durante la erupción del Complejo Volcánico Puyehue-Cordón Caulle 2011- 2012. In *Actas 13°Congreso Geológico Chileno*, (pp. 539-541).

Singer, B. S., Jicha, B. R., Harper, M. A., Naranjo, J. A., Lara, L. E., & Moreno-Roa, H. (2008). Eruptive history, geochronology, and magmatic evolution of the Puyehue-Cordón Caulle volcanic complex, Chile. *Geological Society of America Bulletin*, 120(5-6), 599-618. https://doi.org/10.1130/B26276.1

Spanu A., Vitturi, M. D. M., & Barsotti, S. (2016). Reconstructing eruptive source parameters from tephra deposit: a numerical study of medium-sized explosive eruptions at Etna volcano. *Bulletin of Volcanology*, 78(9), 1-19. https://doi.org/10.1007/s00445-016-1051-2

Steffen, H. (1922). Nachrichten aus den vulkangebieten der Kordilleren von Mittel-Chile. *Zeitschrift der Gesellschaft für Erdkunde zu Berlin*, 273-277

Sulpizio, R. (2005). Three empirical methods for the calculation of distal volume of tephra-fall deposits. *Journal of Volcanology and Geothermal Research*, 145(3-4), 315-336. https://doi.org/10.1016/j.jvolgeores.2005.03.001

Swanson, F. J., Jones, J., Crisafulli, C., González, M. E., & Lara, A. (2016). Puyehue-Cordón Caulle eruption of 2011: tephra fall and initial forest responses in the Chilean Andes. *Bosque*, 37(1). https://doi.org/10.4067/S0717-92002016000100009

Tadini, A., Gouhier, M., Donnadieu, F., de' Michieli Vitturi, M., & Pardini, F. (2022). Particle

Sedimentation in Numerical Modelling: A Case Study from the Puyehue-Cordón Caulle 2011 Eruption with the PLUME-MoM/HYSPLIT Models. *Atmosphere*, 13(5), 784. https://doi.org/10.3390/atmos13050784

Takarada, S., & Hoshizumi, H. (2020). Distribution and Eruptive Volume of Aso-4 Pyroclastic Density Current and Tephra Fall Deposits, Japan: A M8 Super-Eruption. *Frontiers in Earth Sciences*, 8, 170. https://doi.org/10.3389/feart.2020.00170

Toloza, V., Jorquera, C., Mella, M., & Gho, R. (2020). *Peligros del Complejo Volcánico Puyehue-Cordón Caulle, regiones de Los Ríos y Los Lagos*. Carta Geológica de Chile, Serie Geología Ambiental 36, Servicio Nacional de Geología y Minería.

Tormey, D. R., Hickey-Vargas, R., Frey, F.A., & Lopez-Escobar, L. (1991). Recent lavas from the Andean volcanic front (33-42°S): Interpretations of along-arc compositional variations. In Harmon, R.S., & Rapela, C.W., eds., Andean magmatism and its tectonic setting: *Special Paper of the Geological Society of America*, 265, 57-77. https://doi.org/10.1130/SPE265-p57

Van Eaton, A. R., Amigo, Á., Bertin, D., Mastin, L. G., Giacosa, R. E., González, J., Valderrama, O., Fontijn, K., & Behnke, S. A. (2016). Volcanic lightning and plume behavior reveal evolving hazards during the April 2015 eruption of Calbuco volcano, Chile. *Geophysical Research Letters*, 43(7), 3563-3571. https://doi.org/10.1002/2016GL068076

Vergara-Pinto, F., & Marín, A. (2023). Stratigraphy of volcanic memory: Sociocultural dimensions of volcanic risk in the Southern Andes, Chile. *Journal of Contingencies and Crisis Management*, 31(4), 1018–1033 p. https://doi.org/10.1111/1468-5973.12474

Vergara-Pinto, F., & Romero, J. E. (2023). Perceptions of past and future eruptions of Puyehue-Cordón Caulle (Southern Chile): connecting neighbourhood, social cohesion and disaster memory in volcanic risk research. *Revista de Estudios Latinoamericanos Sobre Reducción del Riesgo de Desastres REDER*, 7, 88-110. https://doi.org/10.55467/reder.v7i2.126

Veyl, C. (1960). Los fenómenos volcánicos y sísmicos de fines de Mayo de 1960 en el sur de Chile. Universidad de Concepción, Argentina.

Watt, S. F., Pyle, D. M., Mather, T. A., Martin, R. S., & Matthews, N. E. (2009). Fallout and distribution of volcanic ash over Argentina following the May 2008 explosive eruption of Chaitén, Chile. *Journal of Geophysical Research: Solid Earth*, 114, B4. https://doi.org/10.1029/2008JB006219

Yang, Q., & Bursik, M. A. (2026). new interpolation method to model thickness, isopachs, extent, and volume of tephra fall deposits. *Bulletin of Volcanology* 78, 68. https://doi.org/10.1007/s00445-016-1061-0

Yang, Q., & Jenkins, S. F. (2023). Two sources of uncertainty in estimating tephra volumes from isopachs: perspectives and quantification. *Bulletin of Volcanology*, 85(8). 44. https://doi.org/10.1007/s00445-023-01652-1

Wilson, T., Stewart, C., Bickerton, H., Baxter, P., Outes, A. V., Villarosa, G., & Rovere, E. (2013). *Impacts of the June 2011 Puyehue-Cordón Caulle volcanic complex eruption on urban infrastructure, agriculture and public health*. GNS Science Report, 2012/20. http://hdl.handle.net/11336/78121